Frequency-dependent elastic response at the ferroelectric phase transition of $AgNa(NO_2)_2$

V. P. Soprunyuk,[1] A. Fuith,[2] H. Kabelka,[2] K. Knorr,[1] A. Klöpperpieper,[1] K. Sokalski,[3] and A. V. Kityk[3]
[1]*Fakultät für Physik und Elektrotechnik, Universität des Saarlandes, 66041 Saarbrücken, Germany*
[2]*Institut für Experimentalphysik, Universität Wien, Strudlhofgasse 4, 1090 Wien, Austria*
[3]*Quantum Computer Department, Institute for Computer Science, Technical University of Czestochowa, Aleja Armii Krajowej 17, PL-42200 Czestochowa, Poland*
(Received 1 March 2002; published 4 September 2002)

The elastic dynamics of $AgNa(NO_2)_2$ crystals around the proper ferroelectric phase transition at $T_C = 38°C$ was investigated by ultrasonic ($f = 10$ MHz) and dynamic mechanical analysis (f=0.6-50 Hz) techniques . The system represents a unique example of a ferroelectric crystal with extremely slow dielectric relaxation. Due to this reason it reveals a substantially different elastic behavior in megahertz and hertz frequency regions. We describe our data using a phenomenological model that includes both the effect of order parameter (polarization) relaxation with a characteristic time τ_p and thermal (entropy) relaxation with a characteristic time τ_{th}.

DOI: 10.1103/PhysRevB.66.104102 PACS number(s): 64.70.Kb, 62.20.Dc, 77.80.Bh

I. INTRODUCTION

Structural phase transitions in solids are characterized by the appearance of an order parameter η associated to a certain static distortion of the parent crystal structure. The anomalous behavior of elastic constants in the region of the phase transition is a consequence of the interaction between the order parameter and elastic deformations U_i.[1–3] A coupling linear in deformation ($U\eta^n$ type) gives rise to a *relaxational* contribution to the elastic constants. This is known as the *Landau-Khalatnikow (LK) mechanism*. The LK relaxation contributes to both the real and imaginary parts of the complex elastic constants. The corresponding processes are therefore accompanied by the losses of the elastic energy and are dependent on the actual measuring frequency $\omega = 2\pi f$.[1] Roughly speaking, LK mechanism is the relaxation of the order parameter in the field of dynamic elastic strain. Hence the measurements of the dynamic elastic susceptibility yield important information on the soft mode dynamics. Another mechanisms of the relaxational type may correspond to *domain*,[4,5] *soliton*,[6,7] or *cluster*[8] dynamics. At low frequencies (hertz region) an *entropy (thermal) relaxation* mechanism[9,10,12] appears to be significant in the elasticity of materials. This unusual type of dynamics is the consequence of a heat flow between inhomogenously deformed regions of a sample. The characteristic time of this process is the thermal diffusion time.

Elastic properties can be measured using Brillouin scattering (gigahertz region), ultrasonics (megahertz region), resonance techniques (kilohertz region) and nonresonance methods (hertz region) thus covering a quite broad frequency range. In general, these methods may display different types of the elastic dynamics. In particular, the LK relaxation appears essentially damped if the condition $\omega\tau_\eta \gg 1$ (τ_η is the relaxation time of the order parameter and of the soft mode) is fulfilled. A pronounced elastic softening near the phase transition can, however, occur at low frequencies if $\omega\tau_\eta \ll 1$ and if the coupling between the order parameter and deformation is substantial. In fact this was the reason for the different elastic behavior observed in the Brillouin scattering and ultrasonics experiments for several compounds (see, e.g., Refs. 11 and 12). In most dielectrics the relaxation of the order parameter τ_η is of the order of 10^{-8}–10^{-12} s even in the close vicinity of transition temperature T_C. Thus the LK relaxation is usually well observed in the frequency region up to several hundred megahertz.

The uniaxial ferroelectric $AgNa(NO_2)_2$ constitutes an exception. Its critical Debye-like polarization dynamics appears in the *kilohertz region*.[13,14] The phase transition at $T_C \approx 38$ °C (Refs. 15 and 16) from a paraelectric phase (space group D_{2h}^{24}) to the proper ferroelectric phase (space group C_{2v}^{19}) is due to an ordering of the NO_2^- dipoles.[18] Comprehensive dielectric[13–16] and specific-heat measurements[17] have revealed that the phase transition is of first order, but very close to second order one. The anomalies of dielectric and thermal properties can be well explained by a Landau theory taking into account the near tricritical character of the phase transition. As a consequence the leading term in the free energy expansion is of the sixth order in the polarization P.

In the present paper we report results of an elastic investigation of $AgNa(NO_2)_2$ near the ferroelectric phase transition by using ultrasonic ($f = 10^7$ Hz) and dynamical mechanical analysis ($f = 0.5$–50 Hz) techniques. Due to extremely slow dielectric relaxations one expects substantially different elastic behavior in these two frequency regions. In particular, the characteristic *crossover* of LK relaxation is expected to occur in the kilohertz region quite in contrast to other dielectric materials where this usually appears in the gigahertz region. We describe our data using a phenomenological model that includes both the LK and the entropy fluctuation mechanism. Note that the previous elastic studies of $AgNa(NO_2)_2$ performed by Yamaguchi[19] indeed provide reliable data on the ''clamped'' (decoupled from all relaxational processes) elastic compliances S_{ii}^D, only.

II. EXPERIMENTAL PROCEDURE

Single crystals of $AgNa(NO_2)_2$ were grown from aqueous solution containing 9.8 wt % $AgNO_2$ and 37.2 wt % $NaNO_2$

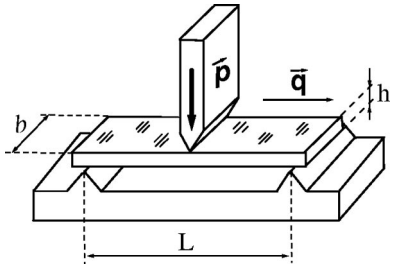

FIG. 1. Three-point bending geometry.

by the slow evaporation method at constant temperature (about 25° C). We used the standard crystallographic orientation for the paraelectric phase: $a=8.05$ Å, $b=10.77$ Å, $c=10.76$ Å. For the ultrasonic measurements the parallel plane samples had a typical thickness of about 3 mm. The longitudinal waves were excited in the sample by $LiNbO_3$ transducers. The wave velocities were measured by the continuous-wave-resonance method[20] in the frequency region 8–12 MHz. The relative accuracy in the ultrasonic measurements was about 10^{-3}.

The low-frequency elastic measurements were performed by the three-point bending method using a dynamic mechanical analyzer (DMA-7, PERKIN ELMER). The sample geometry is presented in Fig. 1. The relation between the effective spring constant k measured by DMA-7 and Young's modulus $Y_{\mathbf{q}}$ is determined by the following equation:[21]

$$k=Y_{\mathbf{q}}4b\left(\frac{h}{L}\right)^3\left[1+\frac{3}{2}\left(\frac{h}{L}\right)^2\frac{Y_{\mathbf{q}}}{G_{\mathbf{pq}}}\right]^{-1}, \tag{1}$$

where $G_{\mathbf{pq}}$ is the shear modulus and the geometrical parameters b,h and L are shown in Fig. 1. Since the values of $Y_{\mathbf{q}}$ and $G_{\mathbf{pq}}$ are of the same order and the ratio $(h/L)^2\approx 0.01$ in our measurements we can neglect the second contribution in Eq. (1). In this case the measured effective spring constant k is proportional to Young's modulus $Y_{\mathbf{q}}$. Since the absolute accuracy in these measurements is usually not better than 20–30% the results are presented in relative units for the real $[\mathrm{Re}S^r_{\mathbf{q}}(T)=\mathrm{Re}S_{\mathbf{q}}(T)/S^o_{\mathbf{q}}(T=60°\mathrm{C})]$ and imaginary $[\mathrm{Im}S^r_{\mathbf{q}}(T)=\mathrm{Im}S_{\mathbf{q}}(T)/S^o_{\mathbf{q}}(T=60°\mathrm{C})]$ part of the effective complex elastic compliance $S^*_{\mathbf{q}}=Y^{*-1}_{\mathbf{q}}$, where $S^o_{\mathbf{q}}=[(\mathrm{Re}S_{\mathbf{q}})^2+(\mathrm{Im}S_{\mathbf{q}})^2]^{1/2}$. The relative units are accurate to within 0.5%. The bending experiment has been performed in the frequency range 0.6–50 Hz at slow cooling with a rate of about 0.1 K/min.

In the three-point bending experiments we used two sample geometries: $\{\mathbf{P}\|[101],\mathbf{q}\|[010]\}$ and $\{\mathbf{P}\|[10\bar{1}],\mathbf{q}\|[101]\}$ that are associated with measuring effective elastic compliances $S_{[010]}$ and $S_{[101]}$, respectively. The compliances are related to the elastic constants C_{ij} by the following equations:

$$S_{[010]}=S_{22}, \tag{2}$$

$$S_{[101]}=(S_{11}+S_{33}+S_{55}+2S_{13})/4, \tag{3}$$

where S_{ij} are the inverse components of the tensor of the elastic constants ($S_{ij}=[C]^{-1}_{ij}$). In the ultrasonic experiments

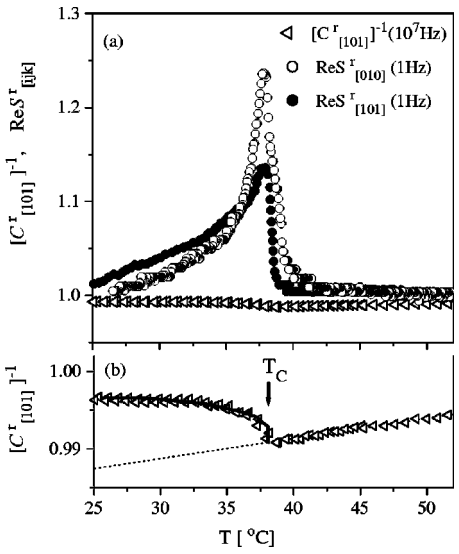

FIG. 2. (a) Temperature variations of $\mathrm{Re}S^r_{[010]}$ and $\mathrm{Re}S^r_{[101]}$ measured by DMA-7 (1 Hz) and the relative temperature changes of the inverse effective elastic constant $[C^r_{[101]}(T)]^{-1}$ measured by continuous-wave-resonance method (10 MHz). (b) $[C^r_{[101]}(T)]^{-1}$ dependence and its fit by P_o^2 (solid line), where P_o is the spontaneous polarization. $P_o(T)$ is taken from Ref. 15.

the quasilongitudinal acoustic waves were exited along the crystallographic [101] direction. The effective elastic constant ($C_{[101]}=\rho V^2$, where ρ is crystal density, V is ultrasound velocity) of this geometry can be expressed through the tensor of elastic constants by solving the Christoffel equation, which gives

$$C_{[101]}=\frac{1}{4}[C_{11}+C_{33}+2C_{55}+\{(C_{11}-C_{33})^2+4(C_{13}+C_{55})^2\}^{1/2}]. \tag{4}$$

III. EXPERIMENTAL RESULTS AND DISCUSSION

Figure 2 shows the relative temperature changes of the real part of the complex effective elastic compliance $\mathrm{Re}S^r_{[010]}(T),\mathrm{Re}S^r_{[101]}(T)$ measured at 1 Hz with the bending technique and the relative temperature changes of the inverse effective elastic constant $[C^r_{[101]}(T)]^{-1}=C^o_{[101]}(T=60°\mathrm{C})/C_{[101]}(T)]$ obtained in the ultrasonic experiment at 10 MHz. In the vicinity of transition temperature T_C a peak anomaly of $\mathrm{Re}S^r_{[010]}(T)$ and $\mathrm{Re}S^r_{[101]}(T)$ is observed. Consequently the temperature dependence of the elastic compliances near T_C measured in the hertz region differs drastically from the ultrasonic data that do not reveal any anomalous peak in the transition region. More precisely, $[C^r_{[101]}(T)]^{-1}$ below T_C is proportional to P_o squared [Fig. 2(b)], where P_o is the spontaneous polarization. The observed elastic behavior in the megahertz region qualitatively quite well reproduces the results of previous elastic measurements[19] for the case of the clamped compliances S^D_{ii}.

The different results obtained at the high and low frequencies can be explained by taking into account that the LK relaxations are suspended in the megahertz region due to the extremely slow dipole relaxation. The anomalies appearing

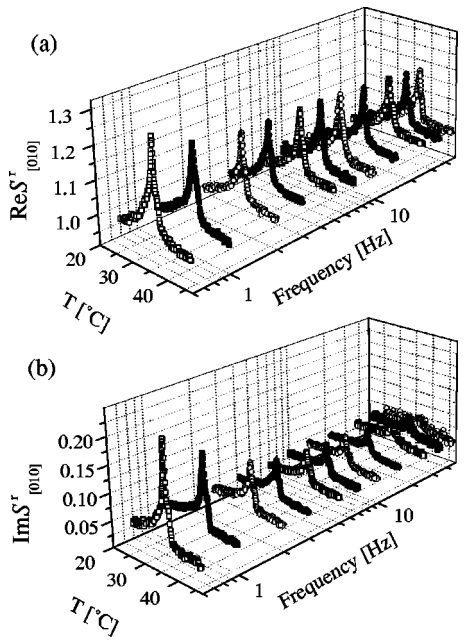

FIG. 3. Temperature dependences of the (a) real $\mathrm{Re}S^r_{[010]}(T)$ and (b) imaginary $\mathrm{Im}S^r_{[010]}(T)$ parts of the effective complex elastic compliance $S^*_{[010]}$ measured at different frequencies.

at low frequencies would be then accounted to the order parameter relaxation which in the hertz region obviously fulfills the condition $\omega\tau_p \ll 1$. However, there is an additional relaxation at very low frequencies as will become clear from the results presented in the Fig. 3 and 4.

Figure 3 shows the temperature dependences of the real $\mathrm{Re}S^r_{[010]}(T)$ and imaginary $\mathrm{Im}S^r_{[010]}(T)$ parts of the effective complex elastic compliance $S^*_{[010]}$ measured at different frequencies (0.6–50 Hz). The anomaly of the real part at T_C is accompanied by a strong maximum of the imaginary part. Assuming that the NO_2 dipoles relax with a single time τ_p

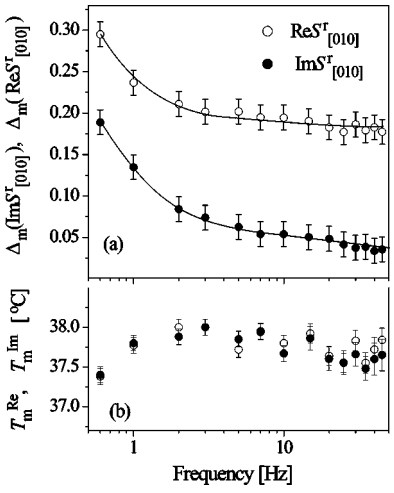

FIG. 4. Anomalous peak height ($T \approx T_C$) for the real $\Delta_m(\mathrm{Re}S^r_{[010]})$ and imaginary $\Delta_m(\mathrm{Im}S^r_{[010]})$ parts of the effective complex elastic compliance $S^*_{[010]}$ (a) and their temperature position T_m^{Re} and T_m^{Im} (b) as a function of driving frequency derived from the data in Fig. 3.

over the full frequency range, the substantial losses that occur in the phase transition region at low frequencies are rather unusual and cannot be attributed to the LK relaxation. Although the LK contribution to the real part of the elastic compliance remains *substantial* and *dominant*, the losses due to the order parameter relaxation at 1 Hz are expected to be about three orders of the magnitude *smaller* compared to what is actually observed in the experiment. Moreover, both the real and the imaginary part manifest strong frequency dispersion (see Fig. 3). As the frequency increases, the anomalous peak in the imaginary part decreases substantially and practically vanishes with the frequency approaching 50 Hz [Fig. 4(a)], whereas the real part decreases only by about 30% reaching a nearly constant value above 3 Hz. At the same time, the temperatures of the maximum real and imaginary parts [Fig. 4(b)] reveal only weak shifts as functions of frequency mainly in the region from 0.6 to 3 Hz. A similar behavior was recently observed near the order-disorder phase transition of KSCN (Ref. 9), C_{60} (Ref. 22), and $(NH_3C_2H_5)_2MnCl_4$ (Ref. 12) and was explained in terms of the LK and heat-diffusion central peak models. We believe that both these mechanisms also apply to the present case. Domain dynamics cannot be responsible for the elastic anomalies observed near T_C. Assuming even domain-wall motion induced by a gradient of deformation (for more detailed description of this mechanism see Ref. 4) the changes of the domain pattern would not contribute to the macroscopic deformations U_i. This is because the expansion of domains with positive polarization and simultaneous contraction of domains with negative one (or vice versa) do not change the macroscopic deformation ($U_i \propto P_o^2$) and therefore do not produce any contribution to the elastic constants.

Let us consider the elastic properties of $AgNa(NO_2)_2$ in the framework of the Landau theory. Taking into account the relations (2)–(4) we will restrict our analysis to the anomalous behavior of elastic constants only. The free-energy expansion considers coupling terms that correspond to anharmonic interactions between the macroscopic deformations U_i ($i=1-6$) and order parameter η. In accordance with group-theoretical analysis the transformation $D_{2h}^{24} \rightarrow C_{2v}^{19}$ is associated with the instability of the dipole active soft mode of the symmetry B_{2u} (Ref. 23) in the center of the Brillouin zone ($\mathbf{k}=0$). Its condensation at T_C leads to the appearance of the macroscopic spontaneous polarization P_o parallel to the crystallographic b axis. Assuming a proper ferroelectric character of this transition, the polarization can be chosen as the order parameter ($\eta \equiv P$). The free energy has the form

$$F = F_P + F_{P,U} + F_U,$$

$$F_P = \frac{1}{2}\Omega_o^2 P^2 + \frac{1}{4}\beta P^4 + \frac{1}{6}\gamma P^6 + \ldots,$$

$$F_{P,U} = \sum_{i=1}^{3} a_i P^2 U_i + \frac{1}{2}\sum_{i,j=1}^{3} b_{ij} P^2 U_i U_j + \frac{1}{2}\sum_{j=4}^{6} b_{jj} P^2 U_j^2,$$

$$F_U = \frac{1}{2}\sum_{i,j=1}^{3} C_{ij}^o U_i U_j + \frac{1}{2}\sum_{j=4}^{6} C_{jj}^o U_j^2, \qquad (5)$$

where $\Omega_o^2 = A(T - T_o)$. Here the P^2U- and P^2U^2-type coupling terms give rise to the relaxational and nonrelaxational elastic contributions, respectively. It is important to note that the bare elastic constant C_{ij}^o in Eq. (5) is usually identified with the adiabatic elastic constants corresponding to the limit $\omega \to \infty$. This is however only valid if the entropy relaxation mentioned in the Introduction is absent. If not, C_{ij}^o must be identified with the low-frequency limit $(\omega \to 0)$, which is with the isothermal elastic constants. Accordingly, two types of the relaxational processes: order parameter $[\delta P(\mathbf{q},t) = \delta P(\mathbf{q},0) e^{-t/\tau_p(\mathbf{q})}]$ and entropy $[\delta T(\mathbf{q},t) = \delta T(\mathbf{q},0) e^{-t/\tau_{th}(\mathbf{q})}]$ relaxations, with the characteristic times τ_p and τ_{th}, respectively, have to be considered in the general case. An isothermal-adiabatic crossover can be reproduced by adding to the free-energy expansion (5) a coupling term $P(0)\delta P(\mathbf{q})\delta T(\mathbf{q})$ (Refs. 9 and 12). Actually, this term is related to a spectrum of temperature fluctuations $\delta T(\mathbf{q})$ that propagate with characteristic diffusion times $\tau_{th}(\mathbf{q}) = (\mathbf{q}\mathbf{D}_{\text{th}}\mathbf{q})^{-1}$, where $\mathbf{D}_{\text{th}}$ is the thermal diffusivity tensor. The characteristic wave vector $\mathbf{q}$ for such fluctuations is defined by the stress profile which in the three-point bending geometry can be approximated by $\sigma(x) \propto \cos(qx)$, where $q = \pi/h \approx 50\ \text{cm}^{-1}$ for the actual sample thickness $h = 0.6$ mm. In principle the value of τ_{th} could be calculated from the thermal conductivity, but unfortunately such data do not exist for the present sample. Referring to tabulated data on other ionic crystals, one expects values between 10 ms and 1 s in the T range of interest.[24] Hence the entropy relaxation is not operational in the megahertz region and ultrasonic elastic constants are always adiabatic. The isothermal-adiabatic crossover can be then obtained by solving simultaneously the equation of motion for the order parameter and the heat conduction equation (Refs. 9 and 10). This gives

$$C_{ij}^o = C_{ij}^{ad} - \frac{C_{ik}^{ad} C_{lj}^{ad} \alpha_k \alpha_l T}{C^{\epsilon}(1 - i\omega\tau_{th})}, \tag{6}$$

where C_{ij}^{ad} are the adiabatic elastic constants, α_k are the thermal expansion coefficients and C^{ϵ} is the isochoric specific heat. Taking into account Eq. (6) and inserting Eq. (5) into the Slonchewski-Thomas equation[1] one obtains

$$C_{ij}^* = C_{ij}^{ad} - \frac{4a_i a_j P_o^2}{\Omega_{\pm}^2(1 - i\omega\tau_p)} - \frac{C_{ik}^{ad} C_{lj}^{ad} \alpha_k \alpha_l T}{C^{\epsilon}(1 - i\omega\tau_{th})} + b_{ij} P_o^2, \tag{7}$$

where $\Omega_+^2 = \Omega_o^2$, $P_o = 0$ at $T > T_C$; $\Omega_-^2 = \Omega_o^2 + (2\beta + \beta')P_o^2 + 5\gamma P_o^4$, $P_o^2 = (-\beta' + \sqrt{\beta'^2 - 4\gamma\Omega_o^2})/2\gamma$ at $T < T_C$; $\beta' = \beta - 2a_i[C^{ad}]_{ij}^{-1} a_j$, $T_C = T_o + 3\beta'^2/16A\gamma$. Expression (7) is the general equation that describes the elastic behavior in the presence of the order parameter and entropy fluctuation. Let us compare this result with the experiment in different frequency regions.

(i) *Megahertz region*. According to Refs. 13,14 the relaxation time τ_p in $AgNa(NO_2)_2$ is in the range (5×10^{-4})–(5×10^{-6})s for the actual temperature interval between 20 and 60°C. For ultrasonic frequencies (10 MHz) $\omega\tau_p \gg 1$ and $\omega\tau_{th} \gg 1$. Therefore both the LK and the entropy relaxations are suppressed. The only possible, nonrelaxational anomalous contribution that can appear under these conditions is due to the last term of Eq. (7). In fact the temperature variation $C_{[101]}^{-1}(T)$ below T_C scales well with P_o^2, as one can see from Fig. 2(b).

(ii) *Region of 50 Hz*. In this frequency region the conditions $\omega\tau_p \ll 1$ and $\omega\tau_{th} \gg 1$ are fulfilled. The response is dominated by the LK mechanism. Remembering that we deal with a nearly tricritical phase transition[13–16] one can put $\beta' \approx 0$. Equation (7) is then reduced to the simple form

$$C_{ij}^* = C_{ij}^{ad}, \quad T > T_C$$

$$C_{ij}^* = C_{ij}^{ad} - \frac{1}{1 - i\omega\tau_p} \frac{2a_i a_j}{2\sqrt{A(T_C - T)\gamma} + \beta}, \quad T \leqslant T_C, \tag{8}$$

which describes the asymmetric peak that occurs in the real and imaginary parts of the complex elastic compliance near T_C (Fig. 3). The anomaly in the imaginary part is expected to be of the order $\Delta_m(\text{Im}S_{[010]}^r) = \omega\tau_p \Delta_m(\text{Re}S_{[010]}^r) \approx 0.15\Delta_m(\text{Re}S_{[010]}^r)$ which is in good agreement with experiment [see Figs. 3 and 4(a)]. Moreover, since $\omega\tau_p(T)$ reaches its maximum value of about 0.15 at T_C, the $\tau_p(T)$ dependence gives only a weak correction (about 2%) to the temperature behavior of the real part of the elastic compliance. Due to this reason also the maxima of the real and imaginary parts do not reveal any substantial temperature shift in the frequency range from 10 to 50 Hz [Fig. 4(b)].

(iii) *Region between 0.6 and 5 Hz*. Both the LK and entropy relaxations are effective in this frequency region, because of the conditions $\omega\tau_p \ll 1$ and $\omega\tau_{th} > 1$. The anomaly of the imaginary part must be attributed to the entropy relaxation only, whereas the real part contains substantial contributions from both relaxational processes. The experiment suggests that the characteristic frequency $f_r = 1/2\pi\tau_{th}$ of the entropy relaxation is in subhertz region. (In principle, it could be shifted to the accessible range of measuring frequencies by reducing of the sample thickness, but our pertinent efforts failed because the crystal easily cleaves along {101}.) Unfortunately, any information concerning the heat conductivity in this crystal is missing in the literature, therefore we cannot estimate quantitatively the relaxation time τ_{th}. A weak temperature shift of the maxima in both the real and imaginary parts of the complex compliance observed in the frequency region 0.6–3 Hz [Fig. 4(b)] must be likely attributed to temperature variations of $\tau_{th}(T) \propto \mathbf{D}_{\text{th}}^{-1} \propto C_p(T)$. Indeed $C_p(T)$ shows strong variations only in a very narrow temperature region (about 0.5°C) around T_C.[17] This explains why the corresponding temperature shifts of T_m^{Re} and T_m^{Im} with a frequency are not substantial in our case.

IV. SUMMARY

We have studied the elastic behavior of $AgNa(NO_2)_2$ crystals by ultrasonic ($f = 10$ MHz) and dynamic mechanical analysis ($f = 0.6$–50 Hz) techniques around the proper ferroelectric phase transition at $T_C = 38$°C. The system represents

a unique example of a ferroelectric crystal with extremely slow dielectric relaxation. Due to this reason it reveals a substantially different elastic behavior in the megahertz and hertz frequency regions. It turns out that in the megahertz region the LK relaxation is fully suppressed. At sufficiently low frequencies ($f<10$ Hz) the elastic behavior clearly indicates the presence of two different relaxational processes. We describe our data using a phenomenological model which considers two relaxational channels, the order parameter (polarization) relaxation with the characteristic time τ_p and the entropy relaxation due to heat transport from the compressed part to the expanded part of the sample with a characteristic time τ_{th}. In this case we assume that no other processes (e.g., interaction of the order parameter with defects, relaxation of mesoscopic cluster, etc.) are involved in the dielectric relaxation in the hertz region. τ_{th} turns out to be of the order of 0.1 s, which appears to be a reasonable value. We hope that these results will find direct support from future measurements of the thermal conductivity and of the low-frequency dielectric response.

[1] W. Rehwald, Adv. Phys. **22**, 721 (1973).
[2] J.O. Fossum, J. Phys. C **18**, 5531 (1985).
[3] R.M. Lynden-Bell and K.H. Michel, Rev. Mod. Phys. **66**, 721 (1994).
[4] A.V. Kityk, W. Schranz, P. Sondergeld, D. Havlik, E.K.H. Salje, and J.F. Scott, Phys. Rev. B **61**, 946 (2000).
[5] A. Binder, K. Knorr, and Y.F. Markov, Phys. Rev. B **61**, 190 (2000).
[6] A.V. Kityk, V.P. Soprunyuk, and O.G. Vlokh, J. Phys.: Condens. Matter **5**, 235 (1993).
[7] A.V. Kityk, V.P. Soprunyuk, A. Fuith, W. Schranz, and H. Warhanek, Phys. Rev. B **53**, 6337 (1996).
[8] P. Kubinec, W. Schranz, and H. Kabelka, J. Phys.: Condens. Matter **4**, 7009 (1992).
[9] W. Schranz and D. Havlik, Phys. Rev. Lett. **73**, 2575 (1994).
[10] W. Schranz, D. Hawlik, and M. Fally Mod. Phys. Lett. B **28-29**, 1817 (1995).
[11] W. Schranz, A. Fuith, H. Kabelka, and H. Warhanek, Ferroelectr. Lett. Sect. **7**, 37 (1987).
[12] A.V. Kityk, W. Schranz, A. Fuith, D. Havlik, V.P. Sopronyuk, and H. Warhanek, Phys. Rev. B **53**, 3055 (1996).
[13] J. Grossmann, D. Muller, J. Petersson, and E. Schneider, Z. Naturforsch. A **31A**, 1089 (1976).
[14] J. Petersson, E. Schneider, and R. Siems, Z. Phys. B: Condens. Matter **39**, 233 (1980).
[15] K. Gesi, J. Phys. Soc. Jpn. **28**, 395 (1970).
[16] K. Gesi, J. Phys. Soc. Jpn. **33**, 108 (1972).
[17] J. Helwig, J. Petersson, and E. Schneider, Z. Phys. B **28**, 87 (1977).
[18] J. Grossmann, D. Muller, and J. Petersson, Z. Naturforsch. A **29A**, 1055 (1974).
[19] K. Yamaguchi, in *Crystal and Solid State Physics, Volume 16 Revise* (Springer-Verlag, Berlin, 1982), Vol. 16, p. 352–355.
[20] W. Schranz and D. Havlik, Phase Transitions **68**, 557 (1999).
[21] D. W. Wilson and L. A. Carlsson, in *Determination of Elastic and Mechanical Properties*, edited by B. W. Rossiter and R. C. Baetzold, Physical Methods of Chemistry (Wiley, New York, 1991), Vol. VII, pp. 180.
[22] W. Schranz, A. Fuith, P. Dolinar, H. Warhanek, M. Haluska, and H. Kuzmany, Phys. Rev. Lett. **71**, 1561 (1993).
[23] O. V. Kovalev, *Irreducible Representations of the Space Groups* (Gordon and Breach, New York, 1965).
[24] W. Schranz (private communication).